AD-A127 234 ASIA RIP: SURFACE WAVE EXPRESSION OF BATHYMETRY(U) 1/1
NAVAL RESEARCH LAB WASHINGTON DC C GORDON ET AL.
23 FEB 83 NRL-MR-5027

UNCLASSIFIED F/G 8/3 NL

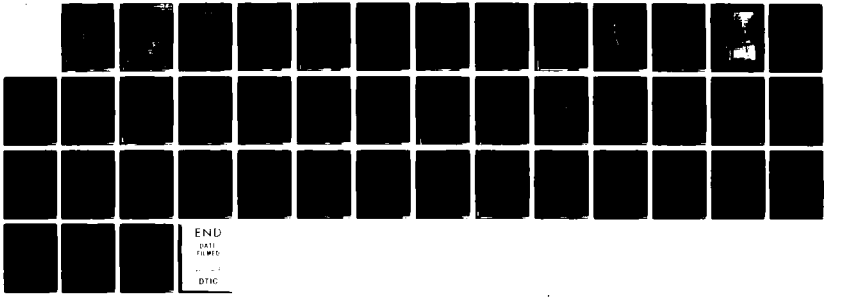

END
DATE FILMED
DTIC

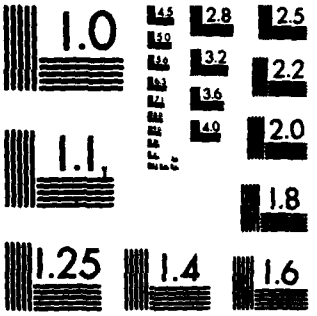

NRL Memorandum Report 5017

Asia Rip: Surface Wave Expression of Bathymetry

C. GORDON AND D. GREENEWALT

Ocean Dynamics Branch
Environmental Sciences Division

J. WITTING

Laboratory for Computational Physics

February 23, 1983

NAVAL RESEARCH LABORATORY
Washington, D.C.

SECURITY CLASSIFICATION OF THIS PAGE (When Data Entered)

REPORT DOCUMENTATION PAGE		READ INSTRUCTIONS BEFORE COMPLETING FORM
1. REPORT NUMBER NRL Memorandum Report 5027	2. GOVT ACCESSION NO. A127234	3. RECIPIENT'S CATALOG NUMBER
4. TITLE (and Subtitle) ASIA RIP: SURFACE WAVE EXPRESSION OF BATHYMETRY		5. TYPE OF REPORT & PERIOD COVERED Interim report on a continuing NRL problem. 6. PERFORMING ORG. REPORT NUMBER
7. AUTHOR(s) C. Gordon, D. Greenewalt and J. Witting		8. CONTRACT OR GRANT NUMBER(s)
9. PERFORMING ORGANIZATION NAME AND ADDRESS Naval Research Laboratory Washington, DC 20375		10. PROGRAM ELEMENT, PROJECT, TASK AREA & WORK UNIT NUMBERS 61153N; RR01310441; 43-1136-0-3
11. CONTROLLING OFFICE NAME AND ADDRESS Department of the Navy Strategic Systems Project Office Washington, DC 20376		12. REPORT DATE February 23, 1983 13. NUMBER OF PAGES 42
14. MONITORING AGENCY NAME & ADDRESS(if different from Controlling Office)		15. SECURITY CLASS. (of this report) UNCLASSIFIED 15a. DECLASSIFICATION/DOWNGRADING SCHEDULE

16. DISTRIBUTION STATEMENT (of this Report)

Approved for public release; distribution unlimited.

17. DISTRIBUTION STATEMENT (of the abstract entered in Block 20, if different from Report)

18. SUPPLEMENTARY NOTES

19. KEY WORDS (Continue on reverse side if necessary and identify by block number)

Current measurements
Topographic effects
Remote sensing
Current-wave interaction

20. ABSTRACT (Continue on reverse side if necessary and identify by block number)

An NRL remote sensing experiment was conducted in July 1982 to measure ocean surface manifestations of subsurface topography and hydrography. The central topographic feature in the operational area was Phelps Bank (40° 50'N-69° 20'W). This report presents the results of current measurements made in the vicinity of Phelps Bank and interpretation of the local surface wave field in terms of wave-current interaction related to the bathymetry.

DD FORM 1 JAN 73 1473 EDITION OF 1 NOV 65 IS OBSOLETE
S/N 0102-014-6601

SECURITY CLASSIFICATION OF THIS PAGE (When Data Entered)

CONTENTS

ASIA RIP: SURFACE WAVE EXPRESSION OF BATHYMETRY

INTRODUCTION

During the past decade wave patterns on the ocean surface have been observed using coherent imaging radar (Brown et al., 1973, 1976; Moskowitz, 1973; Larson and Wright, 1974). Progress in this field has been recently reviewed in detail by Alpers, et al. (1981). This radar imagery is of great interest to oceanographers because the changes in surface roughness responsible for the effect are related to physical oceanographic and meteorological parameters. For example, variations in coherent radar backscatter have been attributed to local wind, surface fronts, ocean swell, internal waves, surface slicks, currents, island shadowing and subsurface topography. The influence of the last of these sources affecting radar imagery is the subject of the SEBEX (surface expression of bathymetry) program initiated by NRL (Valenzuela, 1981; Chen, 1982). This report is an initial interpretation of one surface-wave manifestation of a subsurface topographic feature (Phelps Bank, Nantucket Shoals) based on photographic, bathymetric and current measurements obtained during the NRL Remote Sensing Experiment (pre-SEBEX) aboard the USNS HAYES, July, 1982.

BACKGROUND

The first investigators to note the appearance of subsurface topographic features in the sea-surface imagery of coherent radar (Side-Looking Airborne Radar, SLAR) were DeLoor and Brunsveld van Hulten (1978). They reported that the surface wave pattern had the same crest direction and wavelength as the sand waves on the bottom of the North Sea where their measurements were taken. They tentatively and qualitatively attributed the effect to "interference of the tidal current with the bottom topography

Manuscript approved December 23, 1982.

producing a very weak wave-like pattern which modulates the capillary waves in combination with velocity fluctuations at the sea surface." With regard to the present work they made one particularly relevant observation, that is, no surface manifestations of subsurface sand-wave patterns were detected with turning of the tide, but rather only when diurnal current was present. The implication is that the topographic effect on the surface-wave pattern is probably current related. The infuence of near-surface currents on the wavelengths, amplitudes, speeds and directions of surface waves has been observed and treated theoretically for a long time (Unna, 1942; Johnson, 1947; Taylor, 1955; Ursell, 1960, Longuet-Higgins and Stewart, 1960, 1961). The appearance of current effects in the surface wave field as imaged by coherent radar was first noted by Brown et al. (1976) but no quantitative explanation was offered. Tidal currents in shallow seas and the influence of bottom topography on their radar images has also been discussed in a qualitative way by DeLoor (1981). The explanation proposed by DeLoor (1981) is that "through the tidal current the dune pattern at the bottom modulates the capillary and short gravity waves at the surface which are in resonance with the radar wave". The speculation was based on a comparison of radar imagery with bathymetric charts of the same area, rather than a detailed analysis. The sea depth at the location was about 25 m and the "wave height" of the subsurface sand dunes was about 4 m. The tidal currents involved ranged between 0.5 and 1 $msec^{-1}$.

SLAR imagery of the sea surface in the Southern Bight of the North Sea off the coast of Holland has been reported by McLeish et al. (1981) to reflect sea-floor bed forms such as sand ridges and sand waves. The

sand ridges were the order of 500 m wide and 10 to 25 m below the surface at their crests (Buitenbank, Schouwenbank and Bollen van Goeree). They occur in an area where currents are dominated by rotary tidal components in the range of 0.25 - 0.50 $msec^{-1}$. McLeish et al. (1981) conclude that water depth is the controlling variable responsible for changes in the coherent radar imagery. Basing their interpretation on the "hydrodynamic effect" of ocean waves on radar as proposed by Valenzuela (1978), McLeish et al. (1981) assume that the Bragg waves (order of cm) on the surface that are "seen" by the radar are changed in shape by convergence and divergence of the current flow as it passes over the topographic feature. They suggest that the surface convergence where the sea is deeper tends to increase the density of wave energy whereas divergence over the top of the shallower features will have the opposite effect on wave energy density. It was concluded that the surface manifestation requires two conditions: 1) water flow across a sufficient relative depth change and 2) wind speed sufficient to generate Bragg waves. These investigators also observed that the appearance and disappearance of surface patterns from bottom features depended on the direction of the tidal currents. The features that disappeared in the radar imagery were those roughly parallel to the current direction. As in the earlier work the bathymetry effects on surface waves are associated with current flow.

Some of the most spectacular indications of surface wave patterns reflecting bottom topography have been observed with the SAR (Synthetic Aperture Radar) radar aboard the SEASAT satellite, particularly in the Nantucket shoals area. As yet there are no detailed analyses or interpretations of this data. As pointed out by Phillips (1981) in his discussion

of the SAR imagery and the interaction of short gravity waves with surface currents, there has been little systematic study of the spatial variability of surface currents induced by steady or tidal flow across irregular shallow-bottom topography.

The fact that surface currents interact with gravity waves to change their properties has been the subject of numerous studies. Unna (1942) examined the case in which on shore waves encounter ebbing tidal currents from an estuary at approximately 180° between the directions of current flow and the wave propagation. He found that when waves traveling at speed c meet a current moving at speed u the waves will break when u = -1/4 c regardless of the initial steepness of the wave. Thus in a tidal race or on a bar there can be standing lines of breaking waves and to the leeward of the position where u = -1/4 c the sea will be relatively calm. For example, he found that waves with slack-water wavelengths of 30 m are essentially blocked by a counter current of 1.8 $msec^{-1}$. Johnson (1947) later demonstrated that wave blocking, breaking and refraction may occur even when the waves do not advance directly into the current. His analysis implied that when waves encounter a current of 1.0 $msec^{-1}$, all the waves with speeds less than 10 $msec^{-1}$ (7 sec period) that enter the current at an angle greater than 58° will break and will therefore be unable to cross the current. Johnson (1947) demonstrated the wave-current interaction with a remote sensing experiment using aerial photographs of waves passing through ebb and flood tidal currents at the entrance of Humboldt Bay, California. Taylor (1955) examined this wave-current interaction theoretically for the practical purpose of utilizing the wave blocking phenomenon in designing a "current-flow" breakwater for harbor

protection. He found that for practical purposes the effect was not dependent on the vertical distribution of the current flow. That is, the wave stopping efficiency of a uniform stream is equivalent to that of a stream with a uniform velocity gradient provided the total flow inertia is the same. An interesting example of Taylor's (1955) results is that if a 4.6 $msec^{-1}$ current is present over a sufficiently long distance, it would only have to be 0.5 m deep to stop waves with 30 m wavelengths. More recent work by Longuet-Higgins and Stewart (1960, 1961) and Ursell (1960) has treated the problem of changes in the form of short gravity waves by surface currents in rather rigorous mathematical detail.

FIELD MEASUREMENTS

On July 14, 1982, 1400 U.T. the USNS HAYES was conducting measurements of wave spectra in the vicinity of Phelps Bank, Nantucket Shoals (40°50'N-69°20'W). Two wave-recording buoys were deployed, one free and one tethered to the ship by about 100 m of cable. The ship was adrift with the exception of occasional slow maneuvers to maintain slack cable to the tethered buoy. The ship was carried in a south-westerly direction by the tidal current at a relatively rapid speed (0.8-1.5 $msec^{-1}$) into an area labeled on the charts as Asia Rip (NOAA, 1979). It should be noted that the designation "rip" derives from ripple and implies an area of water made rough by opposing tides or currents. Its presence on a navigational chart also indicates that it is a visible and relatively permanent surface feature. The East to West course of the USNS HAYES over Phelps Bank during the drift into Asia Rip is shown as Track A in Figure 1. As anticipated from the navigational charts, the rip was indeed clearly visible with a rather sharp line of demarcation separating an area of

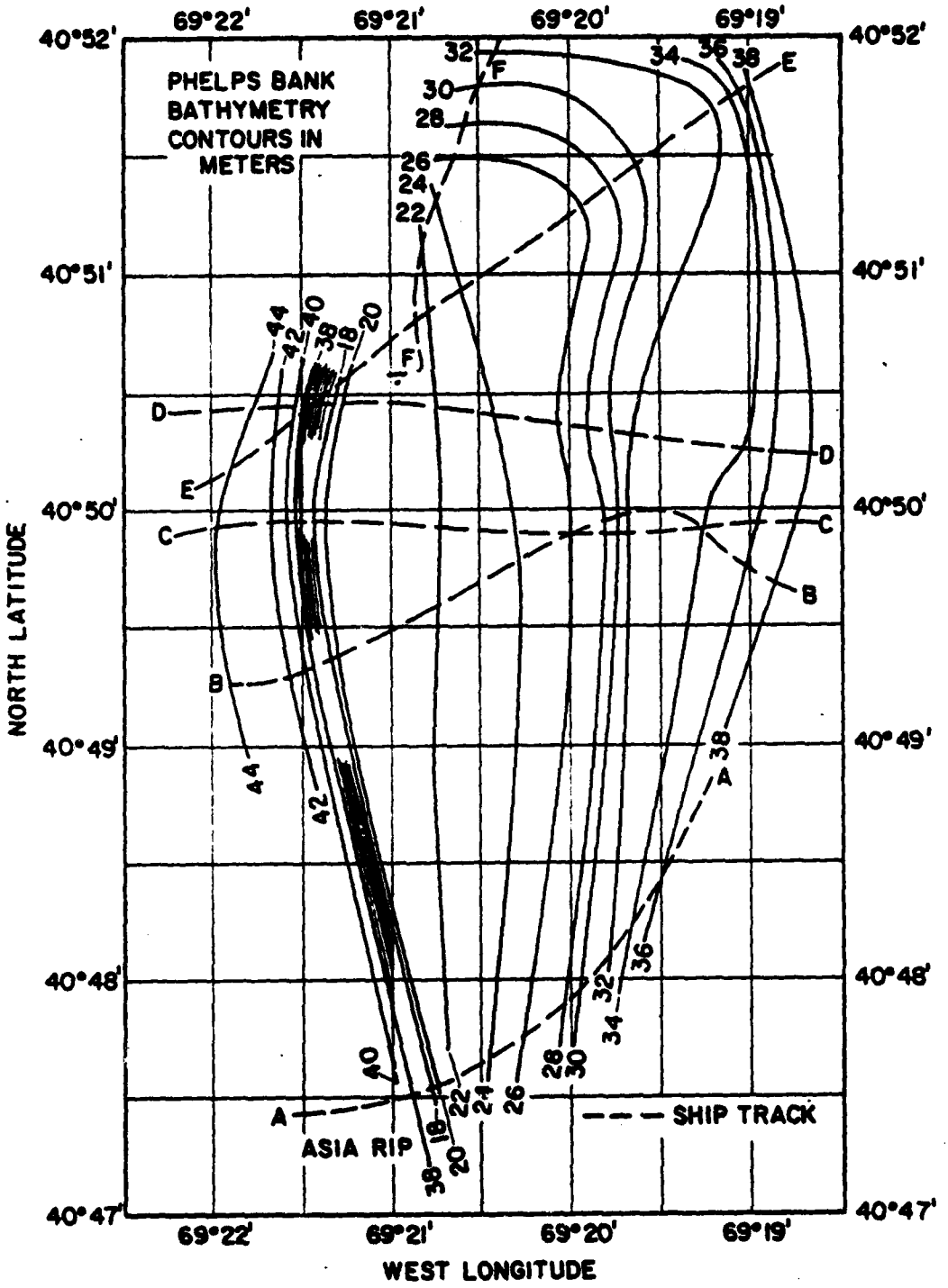

Fig. 1 - The general topography of Phelps Bank based on bathymetric measurements obtained during six ship crossings (Tracks A-F). Asia Rip is located near the southern end of the bank.

considerable wave activity from the relatively calm ambient sea. The photograph in Figure 2 provides a qualitative indication of the change in sea state approaching the rip. The change was roughly equivalent to moving from a sea at about Beaufort scale 2 with small wavelets and a glassy appearance to one at Beaufort scale 3 with large wavelets and some breaking crests. The wind at a height of 10 meters was approximately 5 $msec^{-1}$ at the time. Since neither the meteorological or hydrographic conditions changed significantly as the ship passed into Asia Rip, it was tentatively assumed that the sharp contrast in surface waves was a dynamic effect, probably related to wave interaction with current flow. Because the location of the rip was near the southern end of a prominent, 9 km-long bedform (Phelps Bank, 40°50'N-69°20'W) and inasmuch as the ship course (Track A) showed no sharp directional changes indicating horizontal current shearing, it was decided to pursue the hypothesis that the variations in the near-surface current responsible for the change in wave pattern are related to the bottom topography. In essence then, this is an investigation of a possible SEBEX mechanism (surface expression of bathymetry).

During the at-sea exericse (NRL-Remote Sensing Experiment, July 5-25, 1982) aboard the USNS HAYES, a chart recorder maintained a continuous graphical plot of the depth as measured by a sonic fathometer (EDO Western Corp. 258-E transducer; Raytheon LSR-1811 recorder). Time marks were placed on the bathymetery record by watch standers at intervals varying from a few minutes to a few hours, which made it possibble to calculate the depth at a given time based on the chart recorder speed. Furthermore, navigational information from the LORAN-C system (Northstar Model 7000)

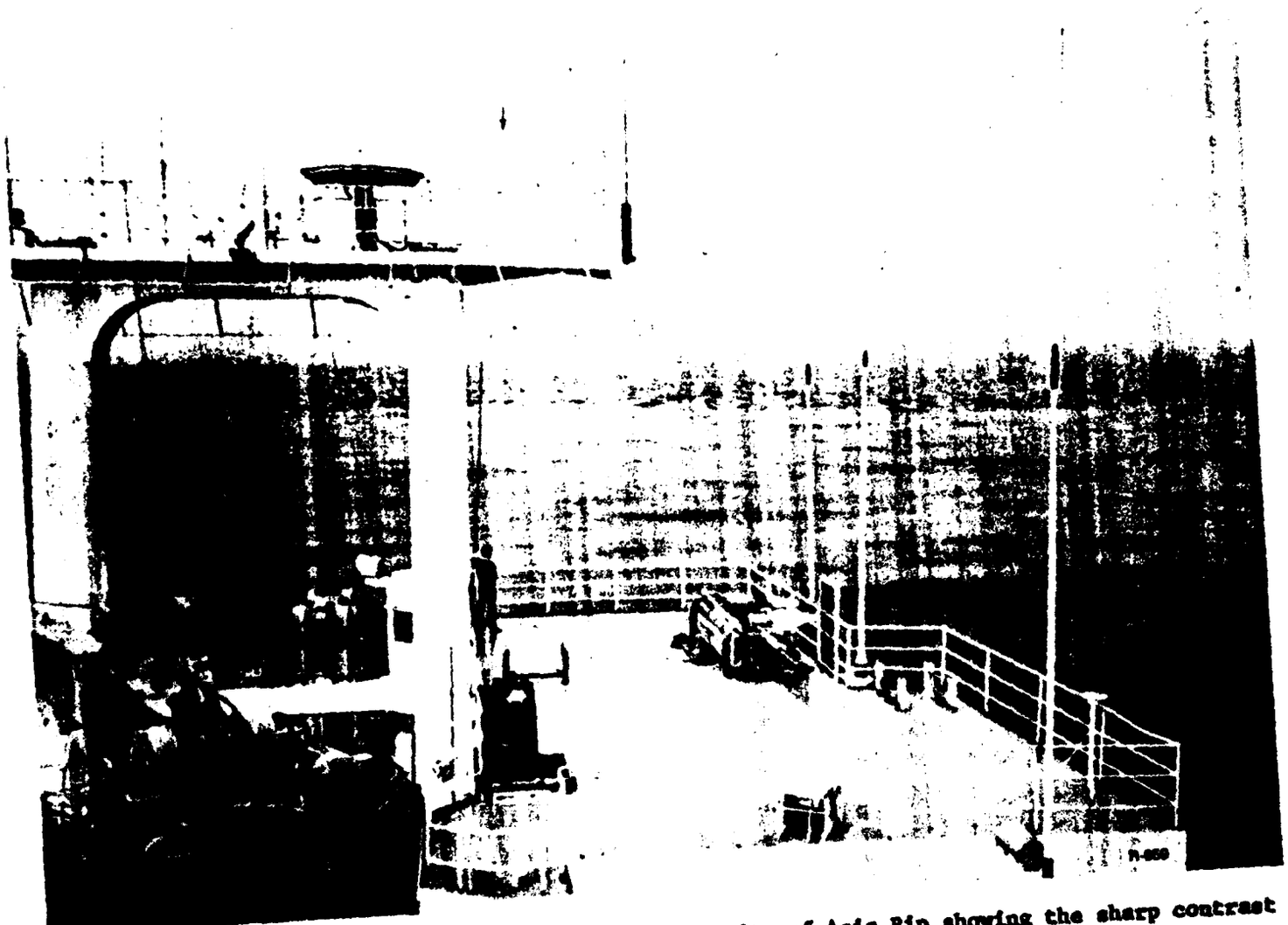

Fig. 2 - A photograph of the sea surface in the vicinity of Asia Rip showing the sharp contrast in surface wave activity. The field of view is directed from Phelps Bank toward the lee side of the feature (west).

was averaged over each minute and logged by computer, providing a time series record of both ship speed and position. By correlating the records for the appropriate times during the cruise it was possible to derive current and bathymetry information at Phelps Bank in general and to relate it to the crossing of Asia Rip in particular.

Table 1. Depths, positions and ship speeds along Track A, July 14, 1982

Time (U.T.)	Speed ($MSEC^{-1}$)	Depth (M)	N. Latitude	W. Longitude
1420	1.62	36.0	40° 48.45'	69° 19.49'
1422	1.73	35.5	40° 48.34'	69° 19.57'
1424	1.74	34.0	40° 48.25'	69° 19.65'
1426	1.65	33.0	40° 48.17'	69° 19.73'
1428	1.50	31.0	40° 48.11'	69° 19.82'
1430	1.42	30.5	40° 48.04'	69° 19.90'
1432	1.36	29.5	40° 47.97'	69° 19.97'
1434	1.25	28.5	40° 47.91'	69° 20.04'
1436	1.22	27.5	40° 47.85'	69° 20.12'
1438	1.29	26.5	40° 47.80'	69° 20.21'
1440	1.34	25.5	40° 47.75'	69° 20.31'
1442	1.34	24.5	40° 47.70'	69° 20.40'
1444	1.28	24.0	40° 47.65'	69° 20.49'
1446	1.23	23.5	40° 47.61'	69° 20.58'
1448	1.19	23.5	40° 47.57'	69° 20.67'
1450	1.20	22.5	40° 47.52'	69° 20.76'
1451.5	——	21.0	Shallowest	Point
1452	1.09	24.0	40° 47.50'	69° 20.82'
1454	0.84	38.0	40° 47.48'	69° 20.89'
1456	0.89	37.5	40° 47.49'	69° 20.99'
1458	1.13	37.5	40° 47.49'	69° 21.09'
1500	1.12	37.0	40° 47.48'	69° 21.18'
1502	1.00	37.0	40° 47.47'	69° 21.26'
1504	0.89	37.0	40° 47.46'	69° 21.33'
1506	0.81	——	40° 47.45'	69° 21.39'
1508	0.28	——	40° 47.44'	69° 21.46'
1510	0.25	——	40° 47.44'	69° 21.53'
1512	0.74	——	40° 47.44'	69° 21.59'
1514	0.76	——	40° 47.43'	69° 21.66'

The navigational and bathymetric data pertaining to the "drift" into Asia Rip is given in Table 1 and shown graphically in Figure 3. The bank profile in the figure represents the recorded depths along Track A plotted in terms of west longitude only. The approximate position of the USNS HAYES at the time of the photograph in Figure 2 is illustrated with some artistic license. The location of the change in surface wave pattern relative to the subsurface topography is presented schematically. The least interpretable information in the figure is the current or ship drift. As mentioned earlier, the ship at the time, was maintaining position relative to a tethered buoy. It was primarily, in a drifting regime, but there is a possibility that some occasional maneuvering took place to accommodate the deployed buoy and there is some ambiguity in the interpretation of the ship speed data. The LORAN-C positions in the area are quite accurate (less than ± 100 m) but the question of the contribution of short-term ship maneuvers to the speed curve remains open. In a qualitative sense, the significant correlation to be gained from Figure 3 is that the change in surface wave pattern coincides spatially with the lee edge of the bank and what appears to be a drop of 30-40 $cmsec^{-1}$ in current speed (assuming that the ship was moving as a Lagrangian drifter at the time).

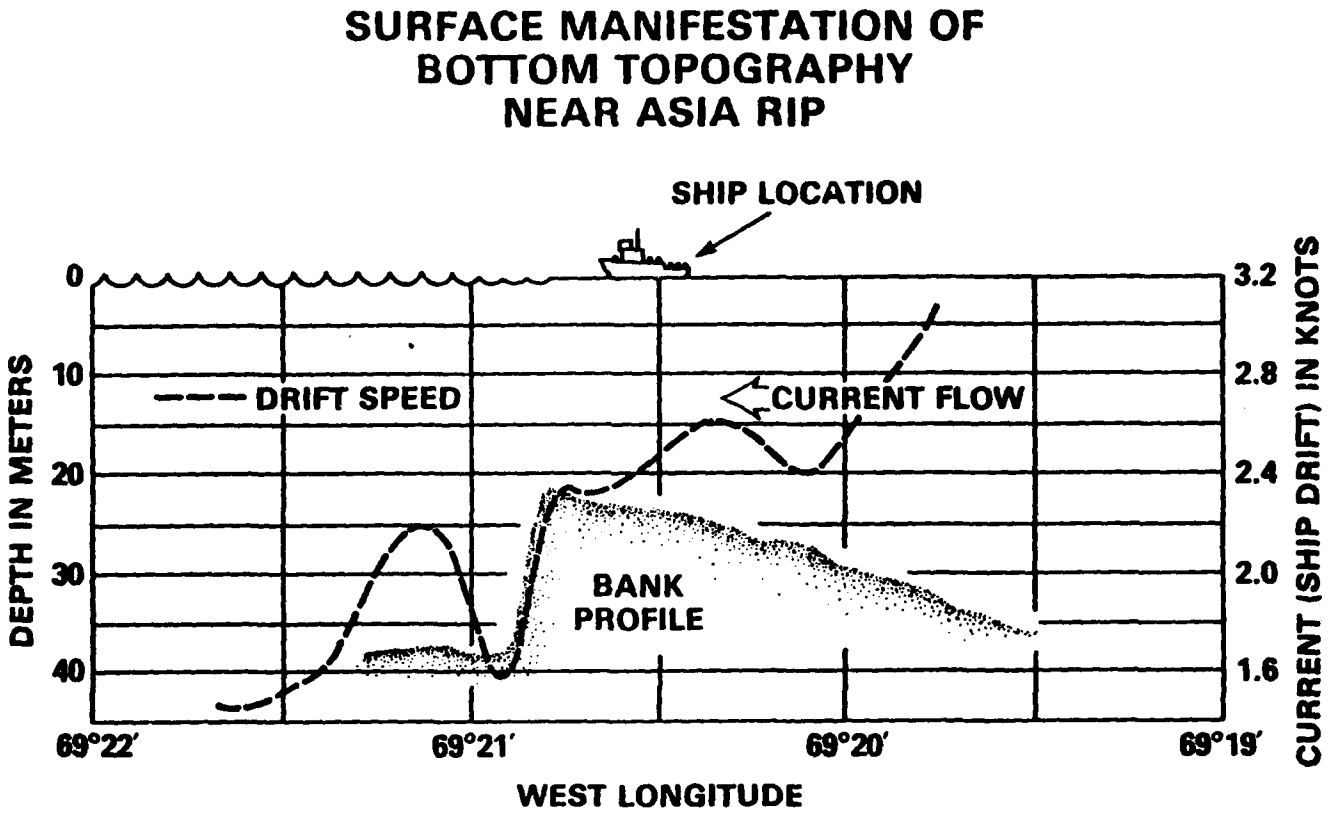

Fig. 3 - A schematic diagram showing the spatial relationship of Phelps Bank, the surface-wave changes and the USNS HAYES at the time the photograph in Fig. 2 was taken. The ship drift speed across the bank is also illustrated. It should be kept in mind that some of the variation in ship speed may be a result of deliberate maneuvers.

Later in the cruise (July 21, 1982) there was an opportunity to repeat an East-to-West ship drift across the bank (Figure 1, Track B) and eliminate the ambiguity associated with possible ship maneuvers. This was done by stopping all engines. Table 2 lists navigational and bathymetric data at two minute intervals for this pass across Phelps Bank. The basic premise in this measurement is that the USNS HAYES (keel depth 5.8 m) acts as a Lagrangian drifter when not under power, that is, the progressive series of LORAN-C fixes recorded aboard ship represent motion of the ocean current only. For this premise to be valid, it must be assumed that no other forces are acting on the ship. The only other force of any consequence would be the wind acting on the superstructure of the ship as a sail. Table 3 provides information on the relationship of the ship course, ship heading and the wind while traversing Track B. It is seen from the table that both the ship heading and the wind speed + direction remained relatively constant during the drift across the bank, that is, the wind remained on the starboard quarter. This is interpreted to mean that the wind effect is constant and if it has any influence, it will be a steady southerly displacement of the ship track. Such an effect could be subtracted out if the ship movement were known as a function of wind speed alone. Therefore, based on this rather qualitative argument, it is considered that the ship drift is probably linearly related to the current.

Table 2. Depths, positions and ship speeds along Track B, July 21, 1982

Time (U.T.)	Speed ($MSEC^{-1}$)	Depth (M)	N. Latitude	W. Longitude
0943	1.09	29.0	40° 49.96'	69° 19.74'
0945	1.03	28.0	40° 49.93'	69° 19.82'
0947	1.01	25.5	40° 49.91'	69° 19.90'
0949	.93	26.0	40° 49.89'	69° 19.97'
0951	.85	25.0	40° 49.88'	69° 20.04'
0953	.82	24.0	40° 49.87'	69° 20.13'
0955	.91	24.0	40° 49.84'	69° 20.21'
0957	.92	23.5	40° 49.81'	69° 20.26'
0959	.88	23.5	40° 49.77'	69° 20.32'
1001	.87	23.0	40° 49.74'	60° 20.39'
1003	.82	23.0	40° 49.71'	60° 20.45'
1005	.86	23.0	40° 49.69'	60° 20.52'
1007	.92	23.5	40° 49.66'	60° 20.60'
1009	.83	23.5	40° 49.63'	60° 20.65'
1011	.77	23.5	40° 49.61'	69° 20.71'
1013	.65	24.0	40° 49.59'	69° 20.77'
1015	.67	23.5	40° 49.58'	69° 20.82'
1017	.76	24.5	40° 49.55'	69° 20.87'
1019	.71	23.5	40° 49.52'	69° 20.94'
1021	.65	22.5	40° 49.50'	69° 20.98'
1023	.65	22.0	40° 49.49'	69° 21.03'
1025	.67	23.5	40° 49.48'	69° 21.10'
1027	.70	24.5	40° 49.45'	69° 21.16'
1029	.69	23.0	40° 49.42'	69° 21.20'
1031	.62	23.5	40° 49.41'	69° 21.24'
1033	.50	22.5	40° 49.41'	69° 21.28'
1035	.50	18.4	40° 49.40'	69° 21.33'
1037	.55	31.5	40° 49.37'	69° 21.37'
1039	.50	37.0	40° 49.36'	69° 21.41'
1041	.36	38.5	40° 49.35'	69° 21.42'
1043	.32	39.5	40° 49.34'	69° 21.46'
1045	.35	40.5	40° 49.33'	69° 21.49'
1047	.35	41.5	40° 49.32'	69° 21.52'
1049	.22	41.0	40° 49.32'	69° 21.54'
1051	.21	41.5	40° 49.32'	69° 21.55'
1053	.26	41.5	40° 49.31'	69° 21.58'
1055	.26	42.0	40° 49.29'	69° 21.59'
1057	.21	41.5	40° 49.30'	69° 21.61'
1059	.10	42.0	40° 49.30'	69° 21.63'
1101	.26	42.0	40° 49.29'	69° 21.66'
1103	.26	42.0	40° 49.29'	69° 21.69'
1105	.26	42.0	40° 49.27'	69° 21.70'
1107	.15	42.0	40° 49.28'	69° 21.71'
1109	.10	42.5	40° 49.28	69° 21.73'

Table 2. Depths, positions and ship speeds along Track B, July 21, 1982 (Cont)

Time (U.T.)	Speed ($MSEC^{-1}$)	Depth (M)	N. Latitude	W. Longitude
1111	.15	42.0	40° 49.28'	69° 21.75'
1113	.21	42.0	40° 49.27'	69° 21.77'
1115	.21	42.0	40° 49.27'	69° 21.78'
1117	.05	41.0	40° 49.28'	69° 21.78'
1119	.05	40.5	40° 49.28'	69° 21.79'
1121	.00	40.5	40° 49.28'	69° 21.81'
1123	.10	40.0	40° 49.29'	69° 21.84'
1125	.10	40.0	40° 49.29'	69° 21.85'
1127	.05	40.0	40° 49.30'	69° 21.84'
1129	.15	40.0	40° 49.31'	69° 21.84'

Table 3. Wind conditions and ship heading during a pass over Phelps Bank (July 21, 1982)

Time (U.T.)	Course (Deg)	Ship Hdng	Wind Speed	Wind Dir
0945			7.3	2.8
0947	246			
0949	250			
0951	256			
0953	257			
0955	254			
0957	250			
0959	237			
1001	233		7.8	326
1003	236			
1005	245			
1007	244			
1009	241			
1011	240			
1013	236			
1015	244	190°	9.5	347.4
1017	245	220°		
1019	237	235°		
1021	238	230°		
1023	248	210°		
1025	257	200°		
1027	242	220°		
1029	236	240°		
1031	243	240°	9.9	354.5
1033	249	220°		
1035	257	220°		
1037	248	235°		
1039	237	235°		
1041	248			
1043	258	220°		
1045	236	240°	9.8	3.9
1047	243	250°		
1049	251	230°		
1051	267	220°		
1053	256	240°		
1055	242	260°		
1057	231	250°		
1059	251	240°		
1101	272		10.4	7.9
1103	251	270°		
1105	234	270°		
1107	246	250°		
1109	286	240°		
1111	264	250°		

Table 3. Wind conditions and ship heading during a pass over Phelps Bank (July 21, 1982)

Time (U.T.)	Course (Deg)	Ship Hdng	Wind Speed	Wind Dir
0945			7.3	2.8
0947	246			
0949	250			
0951	256			
0953	257			
0955	254			
0957	250			
0959	237			
1001	233		7.8	326
1003	236			
1005	245			
1007	244			
1009	241			
1011	240			
1013	236			
1015	244	190°	9.5	347.4
1017	245	220°		
1019	237	235°		
1021	238	230°		
1023	248	210°		
1025	257	200°		
1027	242	220°		
1029	236	240°		
1031	243	240°	9.9	354.5
1033	249	220°		
1035	257	220°		
1037	248	235°		
1039	237	235°		
1041	248			
1043	258	220°		
1045	236	240°	9.8	3.9
1047	243	250°		
1049	251	230°		
1051	267	220°		
1053	256	240°		
1055	242	260°		
1057	231	250°		
1059	251	240°		
1101	272		10.4	7.9
1103	251	270°		
1105	234	270°		
1107	246	250°		
1109	286	240°		
1111	264	250°		

Table 3. Wind conditions and ship heading during a pass over Phelps Bank (July 21, 1982) (Cont)

Time (U.T)	Course (Deg)	Ship Hdng	Wind Speed	Wind Dir
1113	249			
1115	257	270°	10.3	13.5
1117	281	250°		
1119	335	240°		
1121	265	250°		
1123	266	260°		
1125	267	270°		
1127	312	260°		
1129	248	240°		

Note: 1) Ship engines stopped at 0938
2) Wind speed is in meters per second
3) Wind direction and ships course and heading are in degrees
4) Wind speeds and directions are 15 minute averages

The information in Tables 2 and 3 is summarized and correlated graphically in Figures 4 and 5. The bathymetric profile of the bank along the drift track is shown in both figures for common reference. Figure 4 shows a segment of Track B, plotting LORAN-C positions at 4 or 8-minute intervals. The "wind rose" for the duration of the drift is also shown in the figure. It should be noted that the wind remains constant within about ± 25° in direction ± 1.5 $msec^{-1}$ in speed. Figure 5 is equivalent to Figure 3, however there were no accompanying surface wave observations because it was dark and foggy during the pass (Local EDT is 4 hrs earlier than U.T.). The observation of primary interest is the current variation relative to the topography of Phelps Bank. In common with Figure 3, there is a marked change in current (ship drift) speed correlated with the leeward edge of the bank. However, there are fewer large fluctuations in current speed than was the case during the "drift" into Asia Rip (Figure 3). This may be attributable to operating with engines stopped or may indicate that there are fewer turbulent eddies with dimension equivalent to several shiplengths in this area. A particularly noticeable dynamic feature is the rather abrupt change in the East-West current speed (U) gradient around Longitude 69°21.15'. $\frac{dU}{dx}$ undergoes a change of approximately a factor of five at this point. Upstream of the break point $\frac{dU}{dx}$ is 0.14×10^{-3} sec^{-1} while the downstream value is 0.66×10^{-3} sec^{-1}. There is some indication that the current changes are attributable to the bank as such. For example, Figure 5 also includes a current that would be predicted in the absence of any topographic feature. This current prediction is based on Lagrangian measurements that were made west of Phelps Bank during an independent experiment using drogues to follow the trajectory of

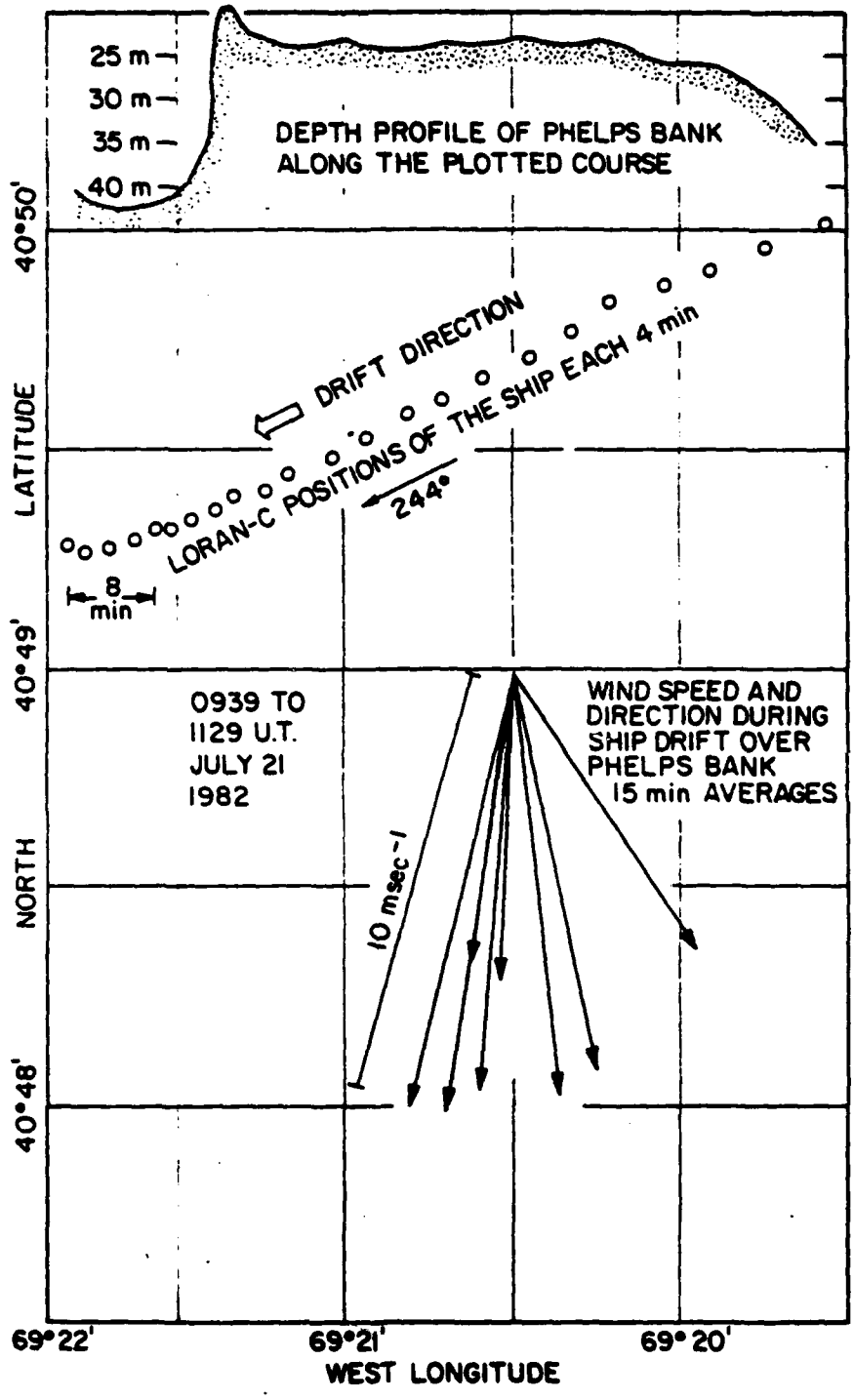

Fig. 4 - Ship drift across Phelps Bank (Track B, Fig. 1). Winds during the drift and the bathymetric profile along the drift path are also shown.

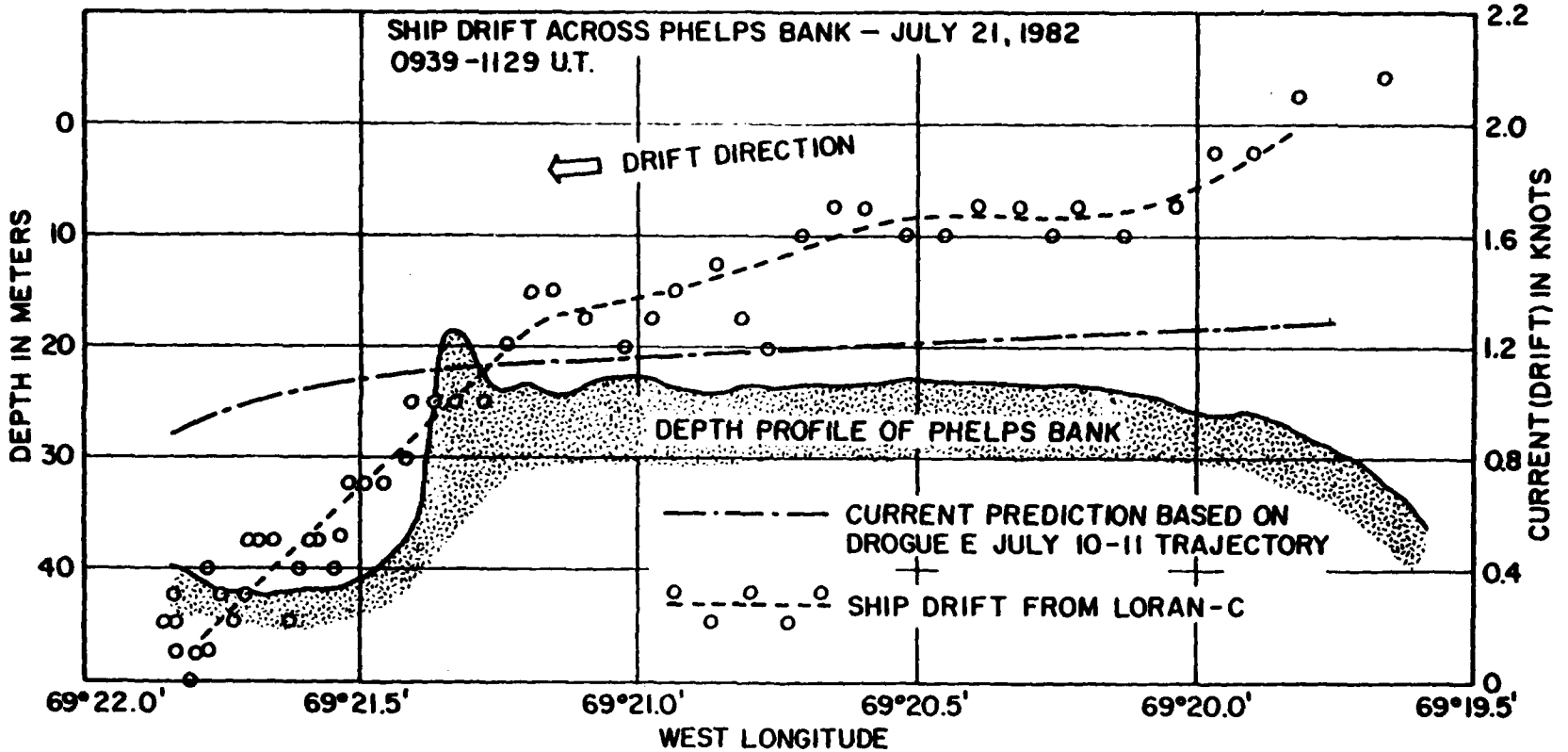

Fig. 5 - The drift speed of the USNS HAYES along the path shown in Fig. 4 (Track B. Fig. 1).

tidal flow in the vicinity. Even though the predicted current may be less than precise, the implication is that current across the shallow part of the bank is faster than would be expected in the absence of the topography while the current in the lee of the sand ridge is slower than anticipated.

In the course of the remote-sensing field exercise there were no other occasions when Phelps Bank was crossed in a drifting mode. During the other East-West passes over the bank shown in Figure 1 (Tracks C,D,E), the ship was under power. If it is assumed that the USNS HAYES was moving through the sea at constant speed (RPM), two of these passes (C and D) do provide some supplementary information on current variation over the bank. During the course of Track C, (ship traveling West to East), the predicted current was flowing East to West (280°) at about 0.5 $msec^{-1}$, that is, the current opposed the ship motion. Data on the ship speed and bathymetry for this track are given in Table 4. The observation of interest is that there is an approximately 0.23 $msec^{-1}$ increase in ship speed as it passes over the lee edge of the bank, an indication of an slower surface current at that location. This is in qualitative agreement with the results of the measurements when the USNS HAYES was in a drifting mode. Analogous information for Track D (Figure 1) is given in Table 5. Here the ship is crossing the bank under power from East to West. The predicted tidal current at the time flows from West to East (125°) and as in the case of Track C, it opposes the ship motion. As seen from Table 5, the ship appears to slow down by approximately 0.34 msec as it passes over the "shallows" of the bank. Since the current opposes the ship's progress, this indicates that the faster current is over the bank with slower currents at both the upstream and downstream edges of the bank. Although

the interpretations of ship speeds under power as current indicators are less reliable than observations in the drifting mode, it should be noted that they are consistent with the drift data.

Table 4. Depths, positions and ship speeds along Track C, July 14, 1982

Time (U.T.)	Speed ($MSEC^{-1}$)	Depth (M)	N. Latitude	W. Longitude
1715	4.97	44.5	40° 49.89'	69° 22.48'
1716	4.72	44.0	40° 49.91'	69° 22.31'
1717	4.54	43.0	40° 49.93'	69° 22.15'
1718	4.53	43.0	40° 49.94'	69° 21.94'
1719	4.65	43.0	40° 49.96'	69° 21.73'
1720	4.72	39.0	40° 49.97'	69° 21.53'
1720.5	———	19.5		
1721	4.76	23.5	40° 49.97'	69° 21.33'
1722	4.65	24.0	40° 49.95'	69° 21.15'
1723	4.58	23.0	40° 49.95'	60° 20.95'
1724	4.51	24.0	40° 49.94'	60° 20.76'
1725	4.48	22.0	40° 49.93'	60° 20.57'
1726	4.52	26.5	40° 49.91'	60° 20.37'
1727	4.54	24.0	40° 49.91'	60° 20.18'
1728	4.54	26.5	40° 49.90'	69° 19.98'
1729	4.54	28.0	40° 49.91'	69° 19.78'
1730	4.52	30.5	40° 49.91'	60° 19.57'
1731	4.52	31.0	40° 49.92'	60° 19.39'
1732	4.55	35.5	40° 49.93'	69° 19.19'
1733	4.54	35.0	40° 49.94'	69° 19.00'
1734	4.57	41.0	40° 49.94'	69° 18.81'
1735	4.59	42.5	40° 49.95'	69° 18.60'

Table 5. Depths, positions and ship speeds along Track D, July 19, 1982

Time (U.T.)	Speed ($MSEC^{-1}$)	Depth (M)	N. Latitude	W. Longitude
1530	4.22	48.0	40° 50.18'	69° 18.10'
1531	4.29	39.0	40° 50.20'	69° 18.28'
1523	4.33	39.0	40° 50.22'	69° 18.47'
1533	4.36	38.0	40° 50.23'	60° 18.65'
1534	4.32	37.0	40° 50.25'	60° 18.82'
1535	4.18	34.0	40° 50.25'	60° 19.00'
1536	4.10	33.0	40° 50.27'	60° 19.17'
1537	4.10	37.0	40° 50.29'	60° 19.35'
1538	4.11	34.0	40° 50.31'	69° 19.53'
1539	4.08	32.0	40° 50.32'	69° 19.69'
1540	4.08	29.0	40° 50.35'	60° 19.87'
1541	4.07	27.0	40° 50.36'	69° 20.04'
1542	4.03	25.0	40° 50.38'	69° 20.20'
1543	3.98	25.0	40° 50.39'	60° 20.37'
1544	3.98	26.5	40° 50.41'	69° 20.54'
1545	3.93	22.0	40° 50.43'	69° 20.72'
1545.3	----	19.5		
1546	3.98	25.0	40° 50.44'	69° 20.89'
1547	4.06	21.0	40° 50.47'	69° 21.07'
1547.3	----	18.0		
1548	4.12	21.0	40° 50.46'	69° 21.24'
1548.2	----	18.0		
1549	4.15	37.5	40° 50.45'	69° 21.43'
1550	4.20	43.0	40° 50.44'	69° 21.62'
1552	4.32	45.0	40° 50.43'	60° 22.00'
1553	4.39	45.0	40° 50.42'	69° 22.19'
1554	4.38	43.0	40° 50.41'	69° 22.38'
1555	4.38	44.0	40° 50.40'	69° 22.56'
1556	4.36	42.0	40° 50.39'	60° 22.75'

Based on these field measurements which are admittedly somewhat limited in both quantity and degree of reliability, the following conclusions can be drawn. Relatively large changes in surface current speed (25 to 50 cm/sec) and current gradient ($0.20 - 1.5 \times 10^{-3}$ sec^{-1}) occur in the vicinity of this topographic feature, with faster currents over the shallow portion of the bedform. The most significant variations in current are spatially correlated with the limits of the bank. The change at the western edge of Phelps Bank was particularly noticeable and on at least one occasion was clearly associated with a sharp contrast in the appearance of the surface wave pattern. It seems reasonable to attempt to relate the surface wave variations to the bathymetry through the mechanism of wave-current interaction. This will be explored in the discussion to follow.

DISCUSSION

For purposes of discussion, we will consider the measurements described earlier in terms of simplified fluid mechanics. Figure 6 is a two-dimensional picture of the fluid mechanical problem. The Figure does some injustice by deletion to the complicated oceanographic situation but includes its essential features. A strong current in relatively shallow water flows over a bathymetric feature and becomes less strong in the deeper water. The water surface in the lee of the feature is covered with waves, some breaking (Figure 2 and Figure 6). The obvious waves are shorter than the water depth (~ 20 m), so we take the relevant water waves to be deep water waves (the depth is infinite for them). At the time of observation (Figure 2) we consider that the waves are directly influenced by the near-surface currents only.*

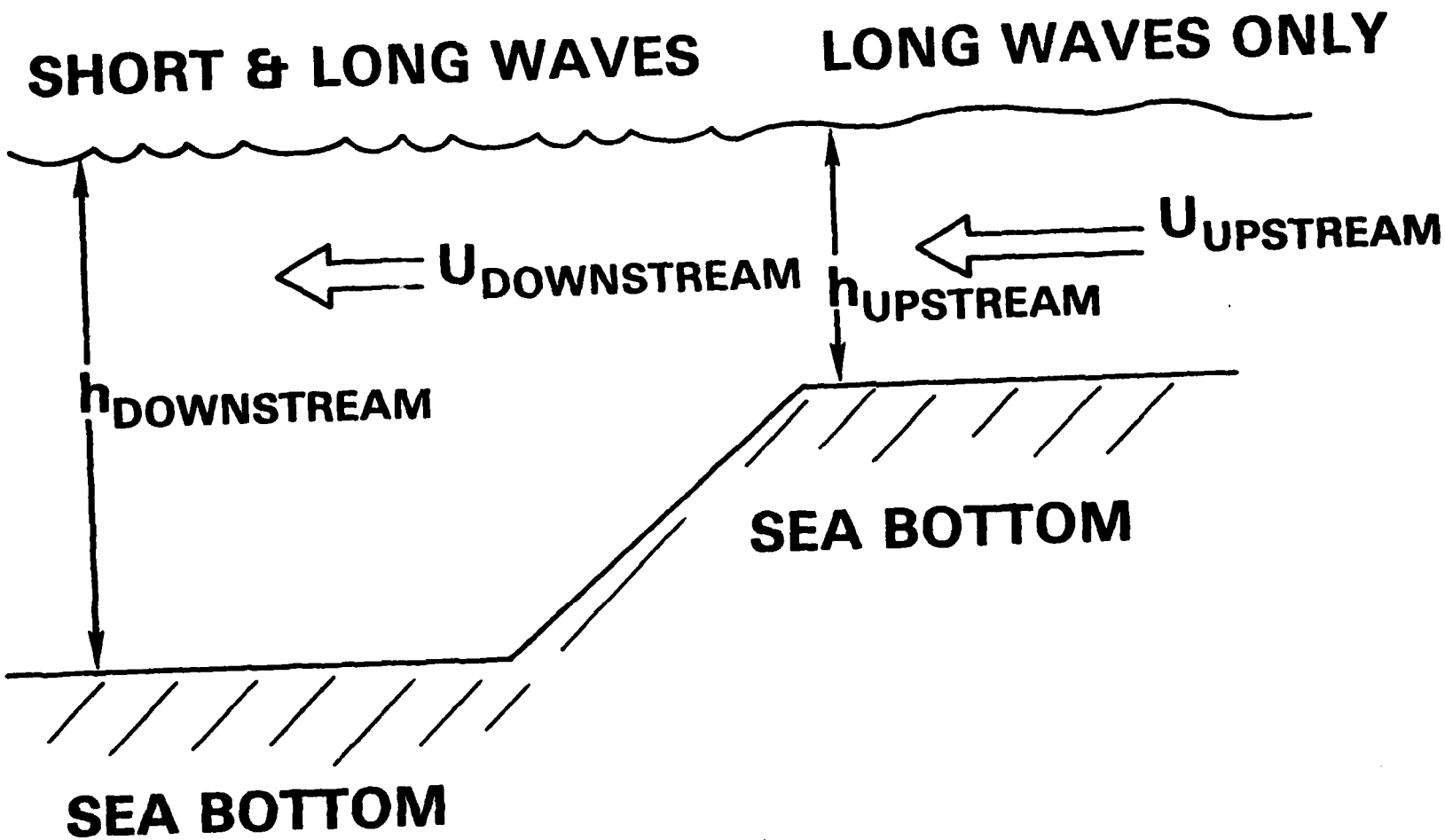

Fig. 6 - A schematic diagram of the fluid dynamic conditions at Phelps Bank.

Two possibilities suggest themselves. Either the variation in current produces the waves, or the currents strongly modify a pre-existing wave field. The former hypothesis is unlikely. While laboratory experience shows that flows encountering discontinuities such as the depth change in Figure 6 can generate waves (hydraulic jumps), this is common only for supercritical flows, i.e., where the upstream speed, $U_{upstream}$, (at the right side of Figure 6) exceeds $\sqrt{gh}_{uptream}$. In these observations, observations, $U_{upstream} \cong$ 1-2 m/sec, while $\sqrt{gh}_{upstream} \cong$ 14 m/sec. The flow is definitely subcritical. Still, to investigate this possibility, we performed a series of numerical calculations using a unified wave model. The computations produced surface current gradients similar to those observed. No spontaneous surface wave generation (beyond that produced by by numerical roundoff errors) was observed. With the proviso that the numerical experiments generated surface current gradients differently (we used a variable channel breadth rather than depth), and ran only to short times (compared to a tidal cycle, the presumed temporal scale of the observed currents; however the run time is long compared to a wave period or likely growth time for the observed waves), we conclude that there is no plausible physical mechanism for generating the observed waves by current gradients alone.

*Slicks must be ruled out as the cause of the change in surface appearance shown in Figure 2 . We do this by qualitatively noting that it is difficult to conceive of a slick that an unpowered ship can float through at a speed the order of 2 kt.

The second possibility, that the currents are modifying the pre-existing wave field to the extent shown in Figure 2, we believe it to be the more likely explanation. Setting aside, for the moment, how the wave field is generated, we will consider the modifications of waves by current. The approach used here is the oldest (Unna, 1942) and is purely kinematic (therefore, reliable). As mentioned earlier, Unna (1942) found that deep water waves traveling directly into a current will be blocked whenever their frequency exceeds a critical value, ω_{crit}. This critical frequency may be identified by:

$$c_{intrinsic} < 4u \qquad (1)$$

where $c_{intrinsic}$ is the speed at which a wave having a frequency ω_{crit} travels in still water (the observations suggest that these are deep-water waves, so there is no ambiguity as to what water is still), and u is the current, assumed to be constant through the water column (our current observations sample the uppermost few meters of ocean, which spans the penetration depth of the obvious waves).

The derivation of Eq. (1) requires: 1) that the currents be steady, 2) that they have gradients only in the direction of the current, 3) that the waves are propagating at a 0° angle of incidence into the currents, and 4) that the waves are "deep water waves," i.e., wavelengths shorter than about twice the depth. In the area of the field measurements the currents are certainly not steady over the course of a tidal cycle. Yet over times appropriate for wave blocking, they probably have a component that is steady enough, plus some fluctuations. That the currents have strong gradients in the direction of the current is borne out by the

shipboard measurements. The assumption of coalignment of wave and current directions, however, is at best speculative and at worst unwarranted. For this reason we present the following derivation of a somewhat more general kinematic theory that removes this restriction, while retaining the assumptions of steadiness and normal current gradients for simplicity, as well as the limitation to deep water waves (well borne out by the observations).

Let us choose the coordinate system in which the currents are most likely to be steady, that is, geographical coordinates, where the bathymetric feature causing current gradients is fixed. The dispersion relation for infinitesimal deep water waves riding in a gradually varying current $u = u(x)$ is:

$$(\omega - k_x u)^2 = gk \tag{2}$$

where ω is the radian frequency of the waves, k_x is the component of wave number aligned parallel to the current u, k is the magnitude of the wave number (2π/wavelength), and g is the accleration of gravity. For the wave field not to generate new waves, and for waves not to break apart across the current gradient we require:

$$\omega = \omega_o = \text{Const}$$
$$k_y = k_{yo} = \text{Const} \tag{3}$$

for a monochromatic, steadily propagating wave train.

In past work it has been customary to define a reference speed $c_o \equiv g/\omega_o$, which is the speed of deep water waves when $u = 0$ (if, indeed, the situation $u = 0$ exists anywhere that steadiness is appropriate; it does not matter, however, because g/ω_o is well defined). In terms of the reference speed (2) leads to:

$$\frac{c^2}{c_o^2} - \frac{u}{c_o} \cos\theta = \frac{c}{c_o} \qquad (4)$$

where θ is the angle between the directions of the current and the wave. Equation (4) is quadratic in c/c_o, and gives:

$$\frac{c}{c_o} = \frac{1}{2} + \frac{1}{2}\sqrt{1 + \frac{4u\cos\theta}{c_o}} \qquad (5)$$

an expression derived by Jonsson et. al. (1970). The other root of (4) is spurious, because it gives zero speed when $u = 0$. Jonsson et. al identify the vanishing of $1 + (4u\cos\theta)/c_o$ as marking wave blocking, and claim that

$$u_{\text{blocking}} = -\frac{c_o}{4\cos\theta} \qquad (6)$$

At this value of u, (5) gives $c_{block} = \frac{1}{2} c_o$. Thus (6) gives:

$$-u_{\text{blocking}} \cos\theta = \frac{1}{2} c_{\text{blocking}} \qquad (7)$$

It should be noted that the wave kinematics represented by equations (2) and (3) are subject to a different interpretation. The singularity of (5) marked by $(4u\cos\theta)/c_o = -1$ turns out not to be singular after all, for a wave does not pass through. Instead, the waves are blocked at different values of (u,θ). We proceed as follows. We nondimensionalize (2) and (3) in the units $\omega_o = g = 1$. Then (2) becomes

$$(1 - k_y u \cot\theta)^2 = k_y \csc\theta, \qquad (8)$$

where k_y is constant along a ray. If, instead of θ, k_x is chosen to be an independent variable, we have:

$$(1 - k_x u)^2 = \sqrt{k_x^2 + k_y^2} \qquad (9)$$

which is, transparently, a quartic equation in $k_x = k_x(u)$ [cubic if $k_y^2 = 1$]. Consequently, there are four k_x's for a particular k_y at each u.

We have solved Eq. (8) to find the relationships between u and θ that correspond to a wave train propagating with the normal component of the energy flux into the current. These are displayed in Figure 7. We should imagine that a wave frequency ω_o is generated at some angle of incidence at a place where the adverse current is u. For simplicity, imagine that u is a monotonic function of x, with $|u|$ increasing upward in the figure. Then the train propagates up one of the solid lines of Figure 7 until it is blocked. This blocking occurs when, at constant k_y, $\partial u/\partial\theta = 0$. Explicitly $\partial u/\partial\theta = 0$ when:

$$|u| = \frac{1}{2}\cos\theta\left(1 - \frac{1}{2}\cos^2\theta\right) \qquad (10)$$

It can be shown that at this point the component of the group velocity parallel to the current equals $-u$. Thus, we interpret blocking as ocurring when the normal component of group velocity matches $|\vec{u}|$. This differs from the interpretation of Jonsonn et. al. that blocking occurs when the component of current parallel to the wave propagation direction matches the group speed.

Above the dashed curve of Figure 7 there can be waves that have phases traveling toward increasing adverse currents; their direction of energy propagation, however, is with the current, and so they cannot be reached from below in the figure.

All waves that start under the dashed curve of Figure 7 arrive at the blocking current having angles of incidence less than $\theta = \cos^{-1}\sqrt{2/3} = 35.3°$, and all have nondimensional blocking currents between 0.2500 and 0.2722. Their wave numbers range between 4.0000 and 2.2500. All waves that start from the abscissa of Figure 7, i.e., are generated in an

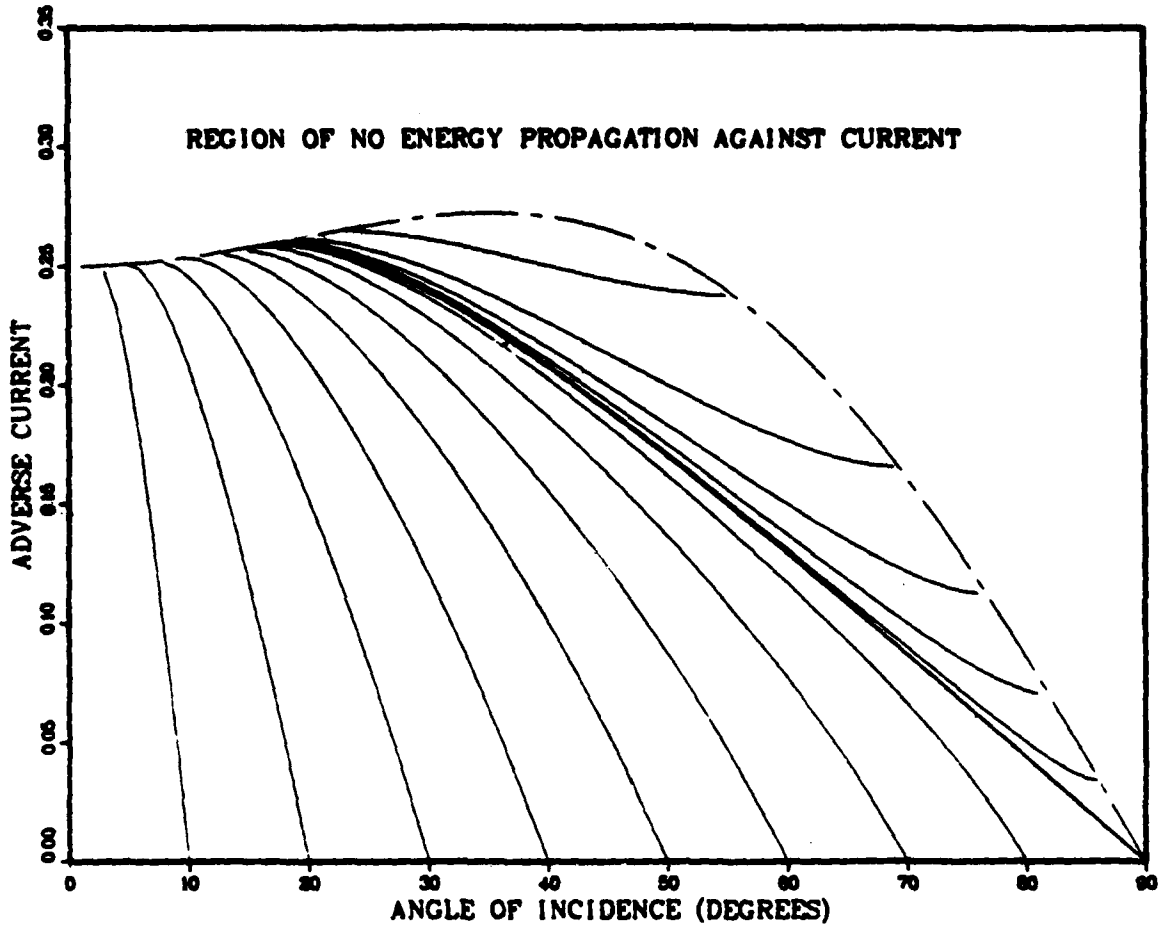

Fig. 7 - Wave blocking trajectories. The adverse current is measured in units of g/ω_o, where g is the acceleration of gravity and ω_o is the radian frequency of the wave. A wave moves up a solid curve, turning into the current until blocked by the current. Below the dashed curve waves can propagate against the current; above the dashed curve they cannot.

We have solved Eq. (8) to find the relationships between u and θ that correspond to a wave train propagating with the normal component of the energy flux into the current. These are displayed in Figure 7. We should imagine that a wave frequency ω_o is generated at some angle of incidence at a place where the adverse current is u. For simplicity, imagine that u is a monotonic function of x, with |u| increasing upward in the figure. Then the train propagates up one of the two solid lines of Figure 7 until it is blocked. This blocking occurs when, at constant k_y, $\partial u/\partial\theta = 0$. Explicitly $\partial u/\partial\theta = 0$ when:

$$|u| = \frac{1}{2}\cos\theta\left(1 - \frac{1}{2}\cos^2\theta\right) \tag{10}$$

It can be shown that at this point the component of the group velocity parallel to the current equals −u. Thus, we interpret blocking as ocurring when the *normal component* of group velocity matches $|\vec{u}|$. This differs from the interpretation of Jonsonn et. al. that blocking occurs when the component of current parallel to the wave propagation direction matches the group speed.

Above the dashed curve of Figure 7 there can be waves that have phases traveling toward increasing adverse currents; their direction of energy propagation, however, is with the current, and so they cannot be reached from below in the figure.

All waves that start under the dashed curve of Figure 7 arrive at the blocking current having angles of incidence less than $\theta = \cos^{-1}\sqrt{2/3} = 35.3°$, and all have nondimensional blocking currents between 0.2500 and 0.2722. Their wave numbers range between 4.0000 and 2.2500. All waves that start from the abscissa of Figure 7, i.e., are generated in an

oceanic region where there are no currents, arrive at the blocking current having angles of incidence less than 17.14°, and all have blocking currents between 0.2500 and 0.2596. Their wave numbers range between 4.0000 and 3.3861.

The observations described here are best interpreted at a given location, where the current has a fixed (and approximately known) value. If wave blocking is occuring at this location, the waves that are blocked must have: 1) an extremely narrow frequency range, 2) a narrow spread of directions near normal incidence to the current, and 3) a rather narrow range of wavelengths. The theory given here makes these predictions even if the wave field has components that originated over a wide range of frequencies and directions. The bounds on these parameters (in dimensional units) are:

$$T_{min} = \frac{2\pi}{g} \frac{u}{0.2772}$$

$$T_{max} = \frac{2\pi}{g} \frac{u}{0.2550} \qquad (11)$$

so for T measured in seconds and u in meters/sec, wave blocking in this theory will be observed in the narrow range of periods:

$$2.3554\ u/(m/sec) < T/sec < 2.5646\ u/(m/sec) \qquad (12)$$

Higher frequency waves (smaller periods) will have been blocked before reaching the observation site, and lower frequency waves (longer periods) can pass through if initially infinitesimal. The ranges of angles of incidence are:

$$|\theta| < 35.3° \qquad (13)$$

The ranges of wavelengths are:

$$2.56\ u^2/(m^2/sec^2) < \lambda/(m) < 3.83\ u^2/(m^2/sec^2) \qquad (14)$$

The wavelengths of blocked waves for specific currents are shown in the table below. The smaller wavelength for each value of current corresponds to a wave at normal incidence while the larger value represents the wavelength when the angle of incidence is 35.3°. These two extremes include the range of wavelengths observed on the surface in the presence of a given blocking current.

Current Speed ($m\ sec^{-1}$)	Range of Wavelengths Blocked (m)
0.25	0.16 - 0.24
0.50	0.64 - 0.96
0.75	1.44 - 2.15
1.00	2.56 - 3.83
1.25	4.00 - 5.98
1.50	5.76 - 8.62

For representative values of u in the measured range of currents encountered in the field (Figs. 3 and 5), that is, 0.75 to 1.25 $msec^{-1}$, (14) yields wavelengths for the blocked waves between 1.44 and 4.00 m for normal incidence and values no larger than 5.98 m for a 35.3° incident angle. This wavelength range is not at odds with qualitative estimates based on visual inspection of Fig. 2. It remains to be demonstrated whether this is quantitively consistent with observations. For purposes of argument we will consider the origin of the waves to be earlier winds.

We have looked at the wind records from the USNS HAYES for the 24 hours preceeding Figure 2, which we call $\tau = 0$ hr. From $\tau = -24$ hr to $\tau = -5$ hr. the wind was blowing with a westerly component at about 10 kt. (5 m/sec). Toward the west, fetch is limited only by the distant continental U.S. which is more than 100 miles away depending on the precise

direction that the light winds traveled. This leads to a fully developed sea. The wind veered clockwise coming from the north at $\tau = -5$ hr., then gradually moving to ENE during the observations. A north-south line marks the boundary between winds from the west (and so before $\tau = -5$ hr.), and winds of essentially infinite fetch, but possibly limited duration (after $\tau = -5$ hr.). Thus, the waves that arrive at the observation site that originated in the west were primarily generated at least five hours before $\tau = 0$.

We will consider 5 m/sec as the windspeed blowing from the west for a long time before $\tau = -5$ hr. Such a wind will produce mostly waves having periods greater than $2\pi c/g = 3.2$ sec. These waves travel at (group) speeds less than 2.5 m/sec; many of the faster (low period) ones will have passed the observation site before the observation (at 2.5 m/sec waves travel 45 km in 5 hours). So at the observation site the majority of waves impinging from the west have periods less than 3.2 sec and speeds less than 5 m/sec. Equation (12) indicates that 3.2 sec period waves will be blocked by currents of about 1.3 m/sec. Considering the uncertainties, this is not inconsistent with the measured currents of Figure 3.

A further complication should be noted. Our knowledge of wave-making by the wind comes from observations where there is little or no current. Presumably, the coordinate system in which the mean current is zero is the one we should use in estimating the frequency content of the wave field (Doppler shifts come into play with any other coordinate system). We have (implicitly) assumed that the wave field's frequency content is that generated by a 5 m/sec wind blowing over a no-current ocean. If substantial

currents flowed during the period of wave generation, the frequency content of the waves when viewed from earth coordinates would differ from those generated in still water. But the waves that arrived from the west at 1442 Z on 14 July 1982 were generated many hours earlier, when tidal currents were, if anything, reversed (semi-diurnal rotary tides predominate in the region). Most of the waves arriving at the observation site in an adverse current were generated during a favorable current, and their frequencies are somewhat higher than waves generated without currents. So our estimate that the dominant wave period of 3.2 sec may be a bit low, and the observed currents of 0.8 - 1.2 m/sec can easily block the dominant wind waves.

CONCLUSION

To summarize our findings, we have observed the striking contrast in ocean surface waves that characterizes a rip. The excess intensity of short waves coincides with the lee side of a bathymetric feature (Phelps Bank). The surface wave effect existed at a time when currents were directed toward the west, where the water is deeper, and when a fossil sea runs toward the east. We have examined some physical mechanisms which may account for this phenomena and find that wave blocking by current is the most likely. Although the conditions may have been especially favorable for wave blocking, the waves having been generated at about 1/2 tidal period earlier, we believe that these observations provide an important clue in interpreting one aspect of SAR imagery.

ACKNOWLEDGMENT

The authors express their appreciation to Dr. Jack A.C. Kaiser for providing most of the meteorological, hydrographic and navigational records used in preparation of this report. We also thank Mr. William Garrett for his photograph of Asia Rip that was used for preliminary wavelength estimates.

We also acknowledge helpful discussions with Dr. Davidson Chen and Dr. Gaspar Valenzuela on wave-current interactions and interpretation of radar imagery of the ocean surface.

REFERENCES

Alpers, W.R., D.B. Ross and C.L. Rufenach (1981). On the Detectability of Ocean Surface Waves by Real and Synthetic Aperture Radar, J. Geophys. Res. 86, No. C7, 6481-6498.

Brown W.E., Jr., C. Elachi and T.W. Thompson (1973). Oceanographic Observation with Imaging Radar, Union Radio Sci. Int. Fall Meeting, Boulder, Colo.

Brown W.E., Jr., C. Elachi and T.W. Thompson (1976). Radar Imaging of Ocean Surface Patterns, J. Geophys. Res. 81, No. 15, 2657-2667.

Chen, D.T. (1982). Surface Effects Due to Subsurface Processes: a Survey, NRL Memorandum Report 4727, January 15, 1-40.

DeLoor, G.P., and H.W. Brunsveld van Hulten (1978). Microwave Measurements over the North Sea, Boundary-Layer Meteorology, 13, 119-131.

DeLoor, G.P. (1981). The Observation of Tidal Patterns, Currents and Bathmetry with SLAR Imagery of the Sea, IEEE Jour. of Oceanic Eng. OE-6, No. 4, 124-129.

Johnson, J.W. (1947). The Refraction of Surface Waves by Currents, Trans. Am. Geophys. Union 28, No. 6, 867-874.

Jonsson, I.G., C. Skougaard and J.D. Wang (1970). Interactions between Waves and Currents, Proc. 12th Coastal Eng. Conf., Am. Soc. Civil Engineers, Vol. 1, 489-507, New York.

Larson, T.R., and J.W. Wright (1974). Imaging Ocean Current Gradients with Synthetic Aperture Radar, Union Radio Sci. Int. Fall Meeting, Boulder, Colorado.

Longuet-Higgins, M.S., and R.W. Stewart (1960). Changes in the Form of Short Gravity Waves on Long Waves and Tidal Currents, J. Fluid Mech. 8, 565-583.

Longuet-Higgins, M.S., and R.W. Stewart (1961). The Changes in Amplitude of Short Gravity Waves on Steady Non-uniform Currents, J. Fluid Mech. 10, 529-549.

McLeish, W., and D.J.P. Swift, R.B. Long, D. Ross and G. Merrill (1981). Ocean Surface Patterns above Sea-Floor Bedforms as Recorded by Radar, Southern Bight of North Sea, Marine Geology, 43, M1-M8.

Moskowitz, L.I. (1973). The Feasibility of Ocean Current Mapping via Synthetic Aperture Radar Methods, Amer. Soc. of Photogramm. Fall Convention, Lake Buena Vista, Fla.

Phillips. O.M. (1981). The Structure of Short Gravity Waves on the Ocean Surface, in Spaceborne Synthetic Aperture Radar for Oceanography, Beal, R.C., P.S. DeLeonibus and I. Katz, editors, Johns Hopkins Univ. Press, Baltimore, Md.

Taylor, G.I. (1955). The Action of a Surface Current Used as a Breakwater, Proc. Roy. Soc. Lond. A 231, 466-478.

Unna, P.J.H. (1942). Waves and Tidal Streams, Nature, 149, No. 3773, 219-220.

Ursell, F. (1960). Steady Wave Patterns on a Non-uniform Steady Fluid Flow, J. Fluid Mech. 9, 333-346.

Valenzuela, G.R. (1978). Theories for the Interaction of Electromagnetic and Oceanic Waves, Boundary-Layer Meteorology, 13, 61-85.

Valenzuela, G.R. (1981). A Remote Sensing Experiment in the Nantucket Shoals (SEBEX), IUCRM Symposium on "Wave Dynamics and Radio Probing of the Ocean Surface," Miami Beach, Fla.; submitted for publication in the proceedings, Plenum Press.

END

DATE
FILMED

6-83

DTIC